TECHNICAL PAPER   TP 2921

High Cycle Fatigue Behaviour of Friction Stir Lap Welded 6061 Aluminium Alloy to Coated Steel Sheet Joint

H. Das · T. K. Pal

Abstract Multi-material fabrication such as joining of steel and aluminium has become prominent now-a-days in automotive industries. Friction stir welding being a novel solid state welding process, has already established good joint strength between steel and aluminium; but fatigue strength of such dissimilar joint has not yet been explored. In the present study, the friction stir lap welding was performed at each rotation speed of 500, 1000, 1500 for two different travel speed i.e. 50 and 100 mm min^{-1} at a constant probe depth of 2.5 mm. Among the six different joints, joint strength achieved of maximum (5 kN) and minimum (2 kN) under two parameter combination i.e. 1000 rpm 50 mm min^{-1} and 500 rpm 100 mm min^{-1} respectively, have been exclusively characterized by high cycle fatigue at R ratio 0.1. Furthermore, R ratio has been varied from +0.5, +0.3 to −0.5, −0.3 at a particular load amplitude which shows the endurance limit (10^6 cycles) for both combination of parameters. The experimental results show that fatigue strength at 10^6 cycles for both the FS welded lap joint is about 20 % of their respective failure load. Thus better fatigue strength is associated with the lap joint performed with the joint of maximum load. The fatigue behaviour of two FS joints has been correlated with the thickness of intermetallic compound and accumulation of dislocations observed by TEM.

Keywords Friction stir welding (FSW) · High cycle fatigue · TEM · Fracture path · R ratio

H. Das · T. K. Pal (✉)
Metallurgical and Material Engineering Department, Welding Technology Centre, Jadavpur University, Kolkata, India
e-mail: tkpal.ju@gmail.com
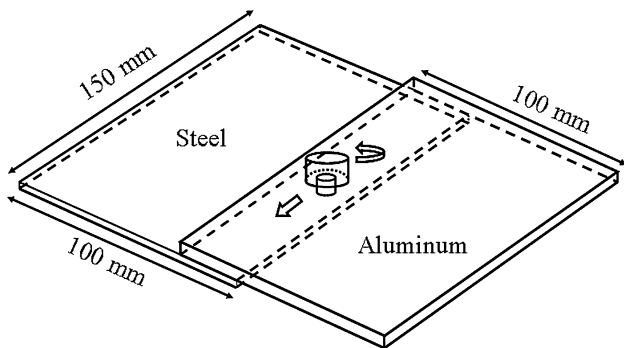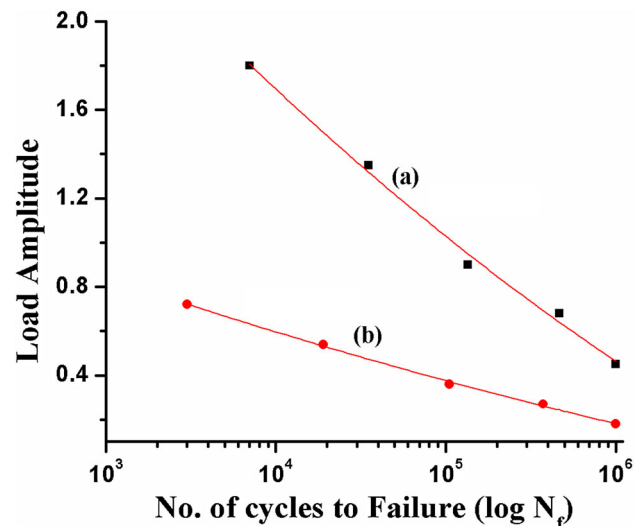
1 Introduction

Recently, the automotive industries are concentrating on multi-material fabrication which can make vehicles much lighter and crash resistant etc. Its adoption in practice is closely linked with the development of efficient methods of joining for dissimilar materials such as steel sheets with aluminium alloys for light weight [1, 2]. But, from practical point of view sound joints between dissimilar materials with low cost fabrication process have to be established [1–3]. Joining of dissimilar metals by conventional fusion welding techniques is very difficult due to large differences in thermo physical properties i.e. melting point, thermal conductivity; thermal expansion which leads to high distortion, residual stresses etc. and also in metallurgical characteristics resulting in the formation of brittle intermetallic phases that generally form by solid state reaction [4]. These intermetallics (IMC) generally results in mechanical degradation of the joint [5, 6]. Friction stir welding (FSW), being a novel solid-state joining process invented by TWI, UK in 1991 has offered excellent welding quality to the joining of aluminum, magnesium etc. over the last decades. With the success in FSW of light metal alloys coupled with lower operating costs due to improved energy efficiency and virtual lack of a consumable has emphasized the need to examine aluminum and coated steel. However, the interfacial region of dissimilar joints produced by FSW is very complicated due to the introduction of complex deformation and the lack of diffusion time leading to formation of very thin intermetallic layer thickness. The analysis of the interfacial region has still remain limited and unclear.

Very few literatures are available globally on FSW of aluminium alloys to coated steel sheet lap joint. The feasibility of friction stir welding of aluminium to steel and

the importance of an Al/steel interface on weld strength has been considered by several authors [7–13]. Few of them reported that to improve the joint strength an IMC layer seems to be necessary; but too thick IMC layer may initiate crack and propagate easily through brittle IMC [11–13]. Bozzi et al. [14] reported optimum IMC layer thickness of 8 μm developed under a rotational speed of 3000 rpm and tool penetration depth of 2.9 mm in friction stir spot welding of aluminium to steel. While making the lap joint of 6063 aluminum alloy (3 mm) to zinc coated steel sheet (1 mm) using FSW, Das et al. [15] reported that failure load as high as 60 % of steel base metal could be achieved. Recent study on lap joint of 6061 aluminium alloy and HIF-GA steel, the authors [16] obtained maximum joint strength 71.4 % of steel base metal with IMC thickness of 6.5 μm.

In any structural design specifically in automotive body structure the high cycle fatigue (HCF) behaviour of welded joints is an important criterion towards the life of the structure. Formation of different zones in FS welded dissimilar joint with distinct microstructural and mechanical properties difference particularly for such dissimilar aluminium and steel friction stir welded joint made the fatigue behaviour more complicated. Although a number of studies have been reported so far on the fatigue performance of friction stir welded aluminium alloys [17–30], study on HCF of dissimilar aluminium and steel friction stir welded joint is meagre. James et al. [31] studied the effect of travel

Fig. 1 Schematic of tool—workpiece configuration for friction stir lap welding. The thickness of steel and aluminium sheets confirm to 1.0 and 2.0 mm, respectively

Fig. 2 S–N curve for a 1000 rpm 50 mm min^{-1} and b 500 rpm 100 mm min^{-1}

Table 1 Chemical composition and mechanical property of coated HIF steel and AA6061

Material	Chemical composition				Mechanical properties		
Steel	%C	%Mn	%Si	%Ti	YS (MPa)	UTS (MPa)	Failure load (kN)
	0.0024	0.47	0.094	0.035	225	375	7.0
Aluminium	%Al	%Si	%Mg	%Fe	YS (MPa)	UTS (MPa)	Failure load (kN)
	98.80	0.52	0.91	0.6	172	295	11.8

Table 2 Process parameter, energy input, failure load and respective process response

Rotation speed (rpm)	Travel speed (mm min^{-1})	Peak temperature (K)	Energy input (kJ)	Avg. Z force (kN)	Avg. torque (Nm)	IMC thickness (μm)	Failure load (kN)
500	50	734.2	88.9	6	15	4.4	2.4
1000	50	801.7	167.89	4.5	12.8	6.5	5
1500	50	829.2	223.8	3.5	11.2	12.6	3.3
500	100	685.2	58.6	7	17	4.1	2
1000	100	704	109.16	5	13.9	5.1	3.2
1500	100	758.6	145	4.5	16	5.5	4.1

Table 3 Load amplitude and No. of cycles to failure at R ratio 0.1

Load amplitude (%)	Load amplitude (kN)	No. of cycles to failure
1000 rpm and 50 mm min^{-1} combination of parameter		
20	0.45	10,00,000
30	0.68	4,67,000
40	0.9	1,35,000
60	1.35	35,000
80	1.8	7000
500 rpm and 100 mm min^{-1} combination of parameter		
20	0.18	10,00,000
30	0.27	3,75,000
40	0.36	1,05,000
60	0.54	19,000
80	0.72	3000

speed on friction stir welding of 5083 aluminium alloy and reported that the occurrence of 'onion-skin' forging-type defects ('kissing bonds') in single pass friction stir (SP FS) welds were generally not associated with fatigue crack initiation, but may act to reduce fatigue life by providing easy linking paths between two fatigue cracks. Fatigue behaviour of friction stir welds of 2024-T3 aluminum alloys were investigated by Zhou et al. [32] and they found that flaws always existed at the roots of FS welds because of unsuitable welding parameters and the fatigue life of flawed welds were 33–80 times shorter than that of flaw-free welds. Lomolino et al. [33] found that naturally aged Al–Mg alloys showed better fatigue properties than that of artificially aged. Cavaliere et al. [34] studied the high cycle fatigue behaviour of 6056 aluminium alloy and reported that fatigue endurance curves show different response of the material as a function of the different processing parameters. Scialpi et al. [35] studied the fatigue performance of 0.8 mm thick dissimilar 2024 to 6082 AA joints by micro (μ) friction stir welding and reported that equiaxed grains in SZ helps to improve the fatigue properties. Das et al. [36] studied the high cycle fatigue behaviour of friction stir butt welded 2 mm thick 6061 aluminium alloy produced under different combination of parameters at R ratio 0.1. Interestingly, the crack path shifted from thermo mechanically affected zone (TMAZ) towards base metal with stress amplitude only at optimized parameter. However, under negative R ratio fatigue life drastically decreased and the crack path remained same for all the
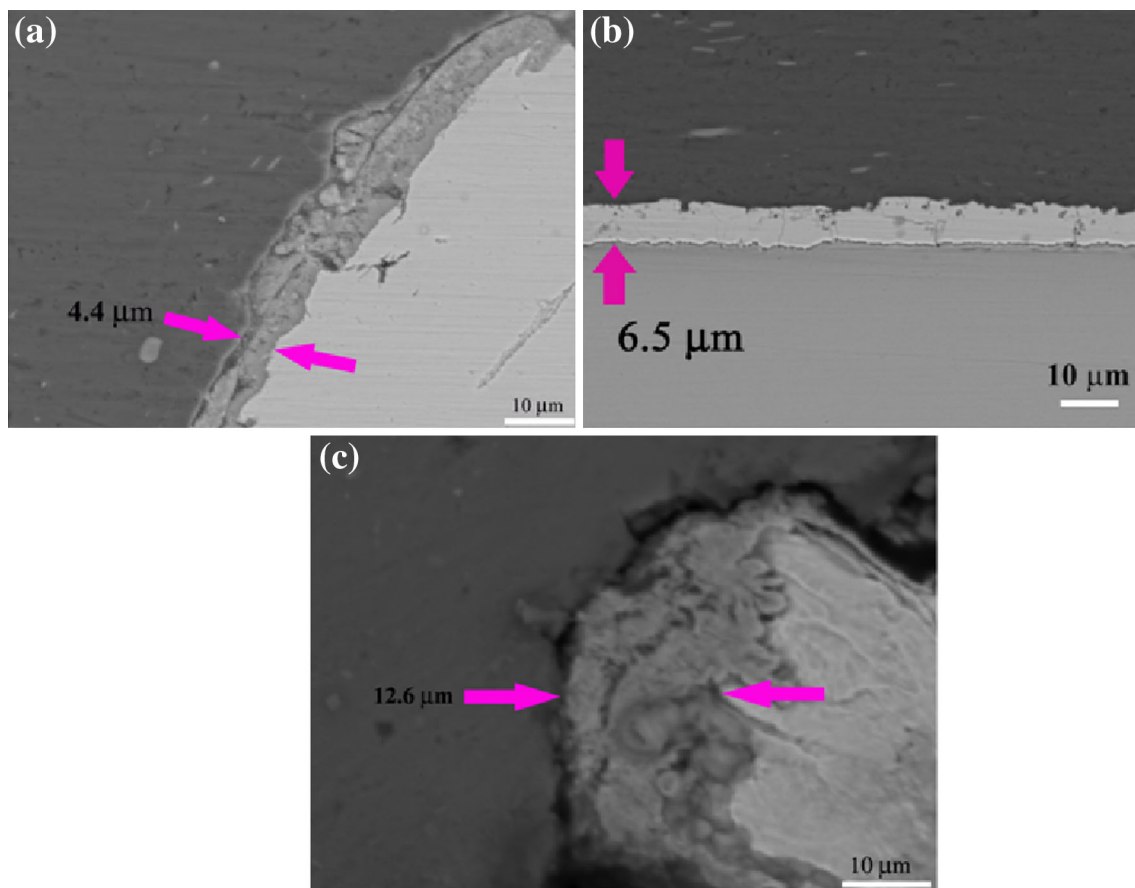
Fig. 3 IMC thickness for **a** 500 rpm, **b** 1000 rpm [16, 43], **c** 1500 rpm at constant travel speed of 50 mm min^{-1}

combination of parameters. Detailed study on fatigue performance of friction stir welded 2024 aluminium alloy was reported by Dalle done et al. [28] and concluded that precipitation sequence plays the most important role on fatigue life. While studying the high cycle fatigue properties of friction stir welded 5083 aluminium alloy Zhou et al. [32], they observed that the cracks initiated from the root of the FS welds, due to the imperfection in the root of weld. Authors felt necessary to detect the flaws for understanding their effects on the fatigue property of FS welds. Fatigue behaviour of friction stir welded and MIG welded 6061-T6 was compared by Moreira et al. [37] and reported that fatigue lives of MIG welded specimens are lower than those of friction stir welded specimens. Niendrof et al. [38] studied the effect of heat treatment on fatigue performance of ultrafine-grained interstitial-free steel and observed that fatigue strength improved significantly with low temperature annealing. Few research papers reported that the determination of the fatigue properties in thin IF steel sheets is extremely problematic due to the high risk of buckling of the sheet during compression [39–41].

In the present study, the high cycle fatigue behaviour of friction stir lap welded 6061 aluminium alloy to HIF GA steel has been investigated. Two joints are considered for HCF—one achieved with maximum load (5 kN) and other with minimum load (2 kN). Both the joints have been exclusively characterized by high cycle fatigue at R ratio 0.1. Furthermore, R ratio has been varied from +0.5, +0.3 to −0.5, −0.3 at particular load amplitude which shows endurance limit (10^6 cycles). The fatigue behaviour of two FS joints has been correlated with the thickness of intermetallic compound and accumulation of dislocations observed by TEM.

2 Experimental

Friction stir welding of 2.0 mm thick AA6061 and 1.0 mm thick high strength interstitial free galvannealed (HIF-GA) steel sheet was performed in lap joint configuration with the AA6061 sheets on the top using a RM Series Friction Stir Welder (Model RM1A-0.7). Schematic of the dissimilar weld is shown in Fig. 1.

The FSW machine can be operated with tool rotational speed up to 3000 rpm, axial load of 67 kN and plunge rates from 0.1 to 1000 mm min^{-1}. The axial force, torque and
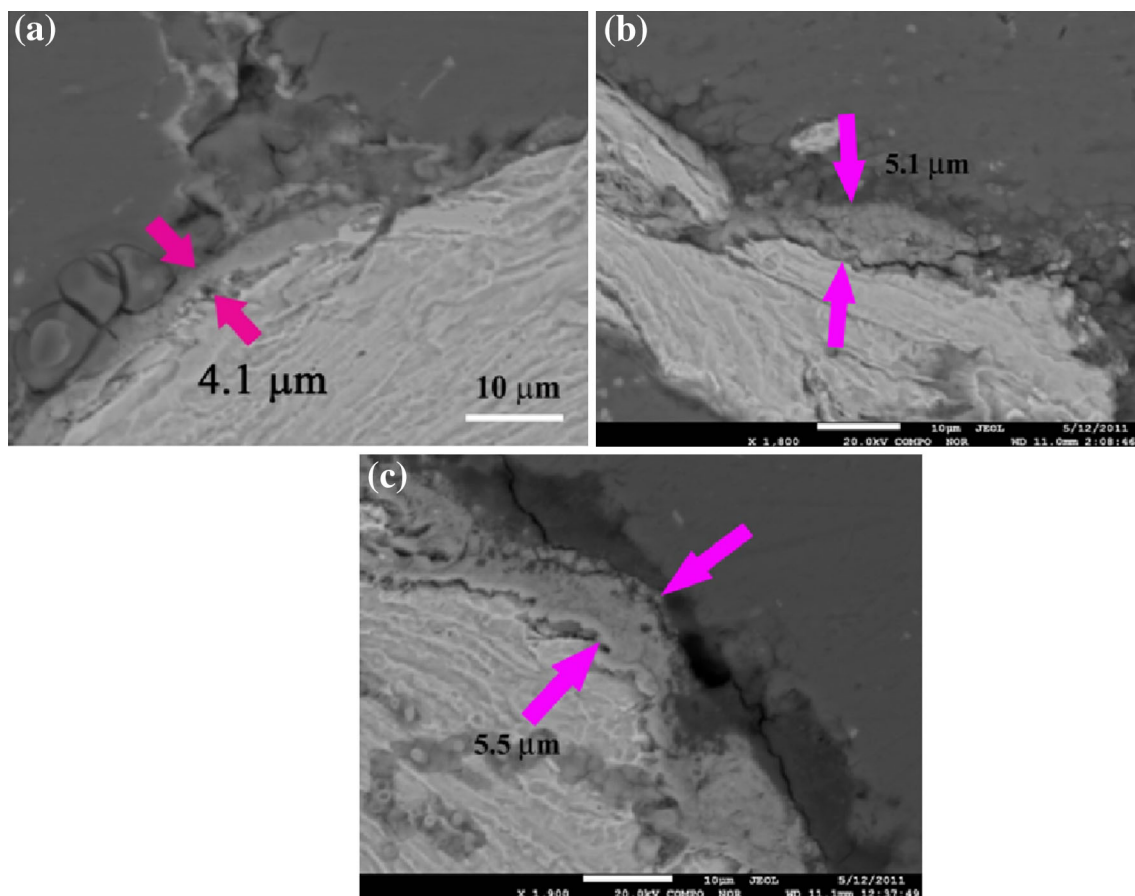
Fig. 4 IMC thickness for **a** 500 rpm [43], **b** 1000 rpm, **c** 1500 rpm at constant travel speed of 100 mm min^{-1}

penetration depth values could be recorded simultaneously during each welding operation with the help of load cell coupled with a data acquisition system. All the lap welds were made under displacement control mode. X force, Y force, Z force and torque were recorded for each joint. The tool used was made of steel SKD61 and comprised of a shank, shoulder (11 mm dia.) and probe. The tool shoulder and the pin diameters are 11 mm and 3 mm, and the pin length is 2.5 mm. The tool was tilted by 2° with the vertical axis in the direction opposite to the welding speed. A dwell time of 2 s after the complete plunging of the tool pin is maintained for all the experiments. Chemical composition and the properties of the base material is shown in Table 1. Table 2 provides the welding conditions (rpm and travel speed) used for the FSLW experiments in the present work with respective energy input, process response (Z force and torque) and failure load.

The energy [42] for FSW was calculated using the following expression and the energy values are summarized in Table 2.

$$\text{Energy} = \int_{t=0}^{t=\text{end of welding}} C_z(t) \times \frac{N_p \times 2\pi}{60} dt \qquad (1)$$

C_z and N_p represents respective torque and rpm.

The weld joint tensile strength was evaluated using transverse tensile specimens of size 180×20 mm in a 100 kN Universal Testing Machine (INSTRON 8862) at a cross head speed of 0.5 mm min^{-1}. High cycle fatigue test was performed in a RUMUL high cycle fatigue testing machine capacity up to 400 Hz. Nanoindentation experiments were carried out using a fully calibrated Nano Indenter XP (MTS Systems) equipped with a standard berkovich indenter. For each loading–unloading cycle, loading and unloading lasted 15 s, respectively, and a dwell time of 30 s at each peak load was used. During each test run, a personal computer collected and stored data for the load and displacement as the indenter was driven into the sample (loading segment) and then withdrawn from it (unloading segment). The raw data were then used to construct the load–displacement plot. TEM was used for the analysis of very thin interfacial areas. TEM observations were carried out using a JEOL-2000EX microscope operating at 200 kV. A 3 mm disc in the relevant area at the centre was punched out from the bulk specimen. The disc was polished down to a thickness less than 100 μm. The interfacial area was then polished down to 20 μm using a Dimple Grinder and diamond pastes. Finally, the interface was thinned by ion beam polishing (GATAN PIPS). Fracture surface of the fatigue specimens were examined under JEOL JSM-8360 scanning electron microscopy to understand the mode of fracture.

3 Results and Discussion

Joint strength for different combination of parameters summarised in Table 2 show highest failure load (5 kN) achieved at 1000 rpm 50 mm min^{-1} and lowest strength (2 kN) achieved at 500 rpm 100 mm min^{-1}. High cycle fatigue study was performed only with these two joints of maximum and minimum strength.

Figure 2 represents (Table 3) the S–N curve of the two welds 1000 rpm 50 mm min^{-1} and 500 rpm 100 mm min^{-1} combination of parameter. It can be observed from Fig. 2 that the weld of 1000 rpm 50 mm min^{-1} has higher fatigue strength than weld of 500 rpm 100 mm min^{-1} considering the fatigue limit defined as the fatigue strength at N = 10^6 cycles.

Formation of intermetallic at the interface plays a decisive role to determine the joint strength for friction stir welding of aluminium-steel dissimilar joint and most importantly intermetallic formation controlled by diffusion process [43]. It is clearly seen from Figs. 3a–c and 4a–c
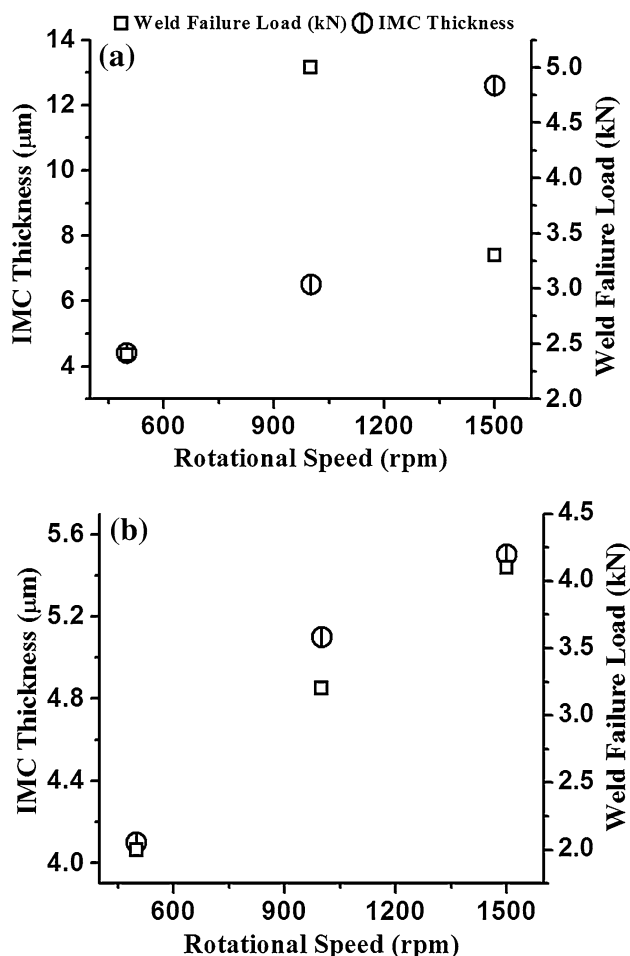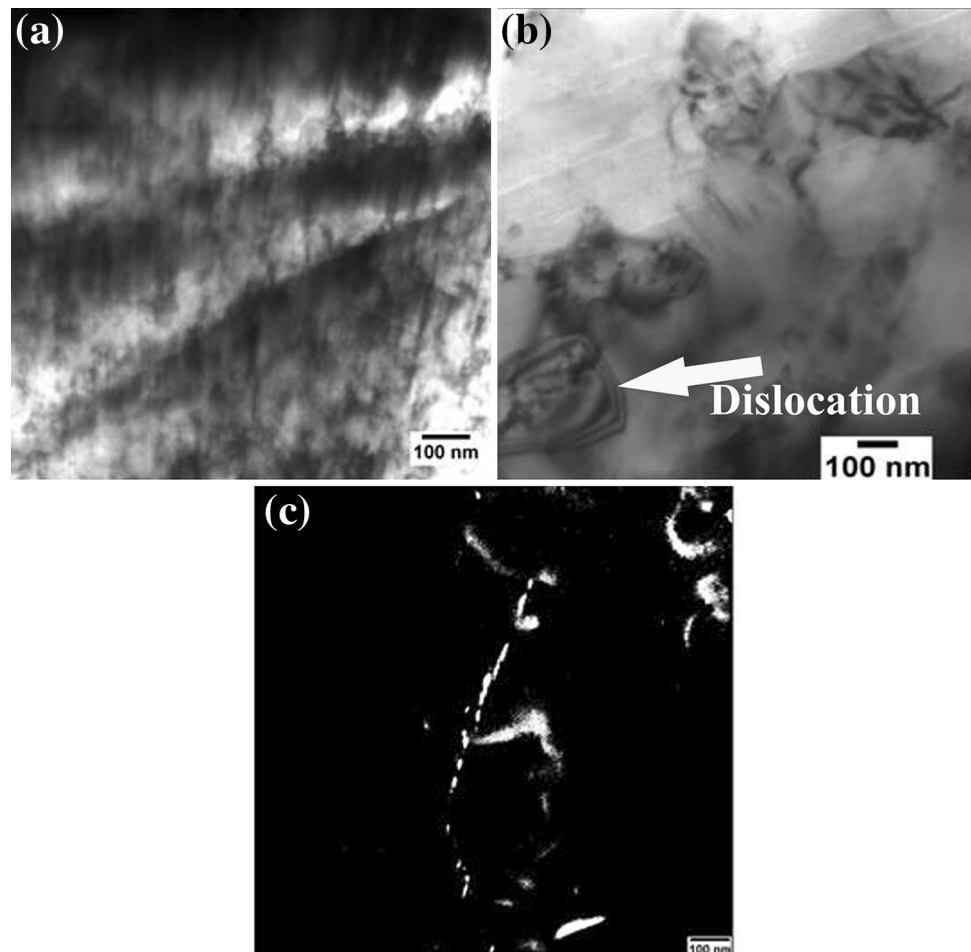

Fig. 5 IMC thickness vis-à-vis weld failure load for different rpm at constant travel speed of **a** 50 mm min^{-1} and **b** 100 mm min^{-1}

Fig. 6 High resolution TEM images of **a** Homogeneous distribution of IMC and **b** accumulation of dislocation for 1000 rpm 50 mm min^{-1} and **c** heterogeneous distribution of IMC for 500 rpm 100 mm min^{-1}

that at constant travel speed of 50 and 100 mm min^{-1}, as the rpm increases from 500 to 1500 IMC thickness also increases. Weld failure load vis-a-vis IMC thickness is shown in Fig. 5. 1500 rpm and 50 mm min^{-1} (maximum energy input of 223.8 kJ) and 500 rpm and 100 mm min^{-1} (lowest energy input 58.6 kJ) shows poor joint strength with maximum and minimum IMC thickness of 12.6 and 4.1 μm respectively. However, 1000 rpm and 50 mm min^{-1} (moderate energy input of 167.89 kJ) combination shows maximum joint strength with IMC thickness of 6.5 μm. This clearly indicates that to improve the joint strength an IMC layer seems to be necessary; but too thick IMC layer may cause easy crack initiation and propagation through brittle IMC resulting poor joint strength.

Furthermore, TEM studies for 1000 rpm 50 mm min^{-1} and 500 rpm 100 mm min^{-1} combination of parameter have been done to understand the distribution of IMC and presence of dislocations. TEM micrographs of the interface region for two different FS welded joint are shown in Fig. 6. Homogeneous distribution of IMC (Fig. 6a) with accumulation of dislocations (Fig. 6b) is evident for 1000 rpm 50 mm min^{-1}. Whereas heterogeneous distribution of IMC shown in Fig. 6c are associated with
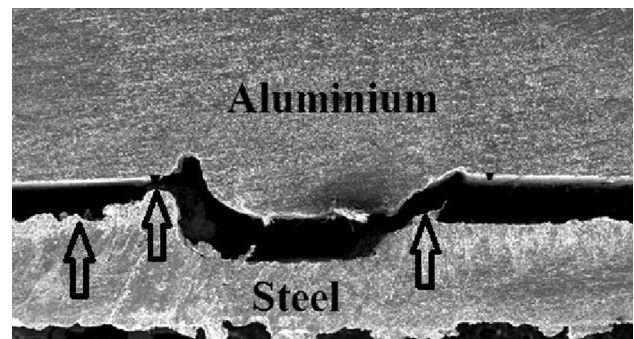
Fig. 7 Interfacial failure at aluminium steel interface

500 rpm 100 mm min^{-1}. The fine distribution of IMC will provide more resistance to crack propagation under both static and dynamic loading conditions leading to improvement of both tensile and fatigue strength.

While studying fracture path during high cycle fatigue test of two joints, different behaviour has been realised. Fracture path (aluminium steel interface) should remain same at all the different loading conditions in case of 500 rpm 100 mm min^{-1} combination of parameter (Fig. 7). Whereas fracture location shifted with the change
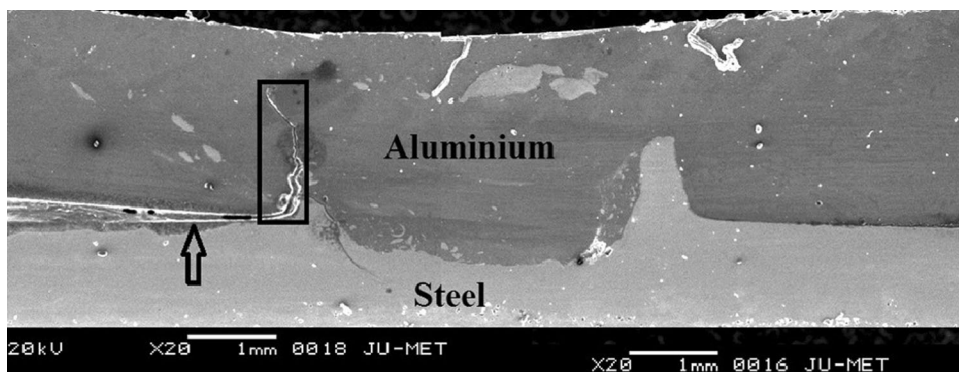
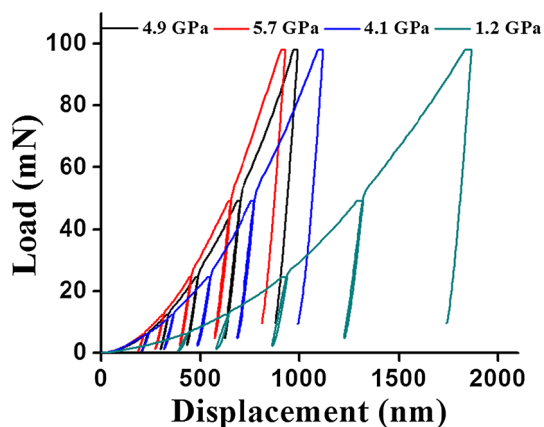**Fig. 8** Crack path at 30 and 40 % of load amplitude for 1000 rpm 50 mm min^{-1}

Fig. 9 Load–displacement curve for 1000 rpm 50 mm min^{-1}

in load amplitude in case of 1000 rpm 50 mm min^{-1}. At 80 and 60 % load amplitude, fatigue fracture occurred at the aluminium steel interface. But, at 40 and 30 % of load amplitude crack at first propagates through the partially bonded joint line and ultimately shifts towards the aluminium side without entering at the Stir Zone (Fig. 8).

Fatigue failure at higher load amplitude (80 and 60 %) occurred similar to tensile failure i.e., at the joint interface for both combination of parameters. This is mainly due to formation of IMC with very high hardness (Fig. 9) and brittle in nature. In such aluminium steel dissimilar friction stir welded joint, fatigue crack easily initiates from the partially bonded joint line at both higher and lower load amplitude. But at higher load amplitude, crack has got sufficient energy to follow the least resistance path i.e. the interface of the stir zone which is the most brittle path. On the other hand, for 1000 rpm 50 mm min^{-1} travel speed at a relatively lower load (40 and 30 %) crack will not get sufficient energy to cross the barrier (portion formed at the two corner of "U" shaped stir zone); rather struck off at the corner of "U" shaped stir zone and finally propagates through comparatively softer aluminium side (Fig. 6). However, it is to be noted that such crack propagation behaviour is not observed in case of 500 rpm 100 mm min^{-1}. This result indicates that crack even with insufficient energy (lower load amplitude) has been able to propagate through the interface due to lower bond strength.
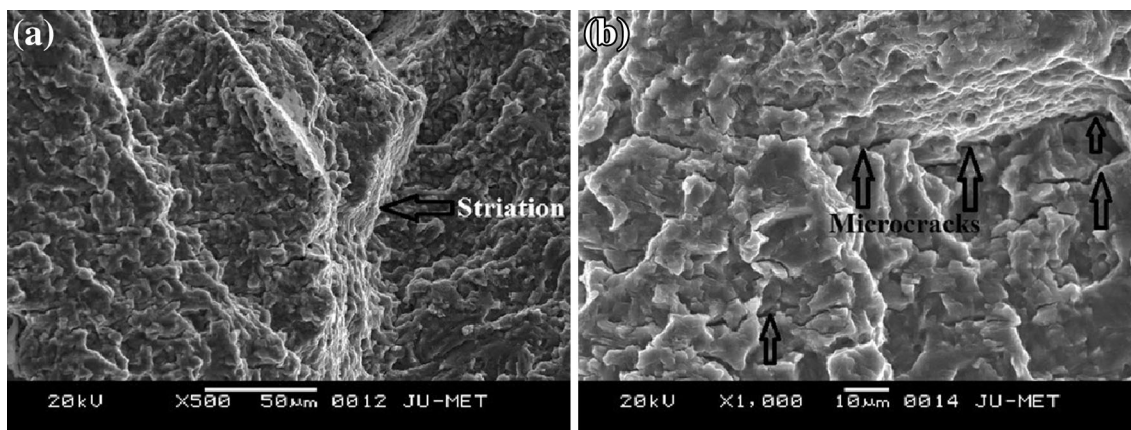

Fig. 10 Fracture surface at **a** 30 % of load amplitude and **b** 40 % load amplitude for 1000 rpm 50 mm min^{-1}

Table 4 R ratio, load amplitude and no. of cycles to failure

R ratio	Load amplitude (kN)	No. of cycles to failure
1000 rpm and 50 mm min^{-1} combination of parameter		
0.5	0.35	10,00,000
0.3	0.25	10,00,000
−0.5	0.75	1,55,000
−0.3	0.65	4,75,000
500 rpm and 100 mm min^{-1} combination of parameter		
0.5	0.1	10,00,000
0.3	0.14	10,00,000
−0.5	0.3	1,15,000
−0.3	0.26	3,72,000

Nanoindentation test has been carried out for better understanding the impact of IMC hardness on failure path for 1000 rpm and 50 mm min^{-1} combination of parameter. Close look into the nanoindentation curve (Fig. 9) clearly shown that the resultant unloading and reloading curves are nearly coinciding for 1, 2 and 3 indicating elastic behaviour. Whereas distinct hysteresis loops for point 4 was observed in unloading–reloading cycles, indicating reverse plasticity. Results are expected because indentation 4 (122.5 HV) represent steel which has undergone deformation. On the other hand, the nano hardness values at other different points such as point 2 (582Hv) for $Al_{13}Fe_4$, point 1(498 Hv), 3(08Hv) for Fe_3Al represent the zone of non-deformation. Under lower load condition due to lower
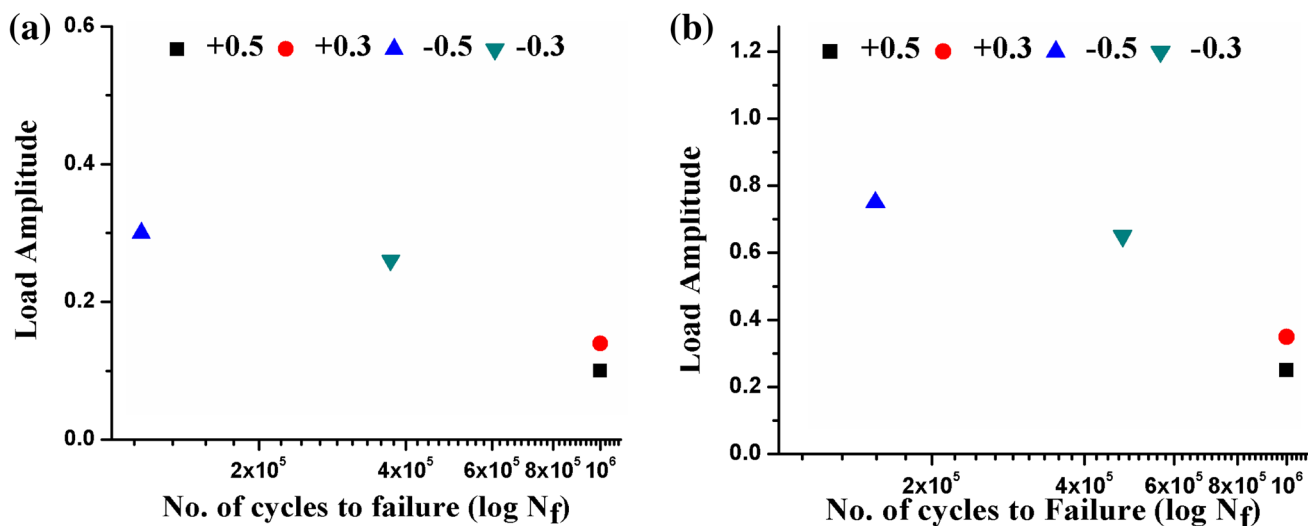
Fig. 11 Effect of R ratio on endurance limit for **a** 1000 rpm 50 mm min^{-1} and **b** 500 rpm 100 mm min^{-1}
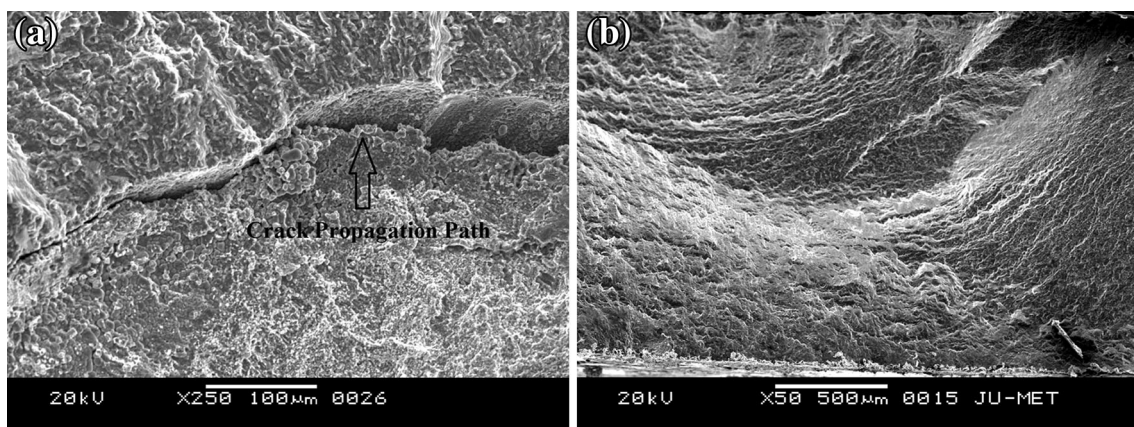
Fig. 12 Fracture surface at negative R ratio

energy of the crack path, crack cannot propagate through the hardened intermetallic rich interface of the joint.

Lower volume fraction of IMC in lower strength joint (500 rpm 100 mm min^{-1}) than high strength joint (1000 rpm 50 mm min^{-1}) has probably failed to restrict the crack propagation and thus fracture path remains unaltered.

Fracture surfaces are uneven and non-homogeneous. Typical striation marks are observed on the fracture surface of 30 % load amplitude and number of micro cracks are observed in the fracture surface of 40 % load amplitude shown in Fig. 10a, b.

During high cycle fatigue testing R ratio were varied from −0.5, −0.3, 0.5 and 0.3 at 20 % of load amplitude (endurance limit) (Table 4). It is interesting to note that both the joints with negative R ratio i.e.−0.3 and −0.5 show decrease in fatigue life at 20 % of load amplitude (Fig. 8), whereas fatigue life remains unaltered at 10^6 cycles with R ratio of 0.3 and 0.5 at 20 % of load amplitude for both the joints (Fig. 11). In all cases, however, interfacial type of failure has been occurred. With higher negative ratios, it become more difficult to find striations probably due to abrasion and no. of micro cracks with a clear crack propagation path has been observed (Fig. 12). The experimental results, however, suggest that under spectrum loading conditions the negative portion of a loading spectrum cannot be neglected. It is reported that the plastic zone size, however, can be drastically altered by subsequent cycling, particularly with negative R ratio [44]. Thus, the significance of the reversed stress plastic zone is subsequently reduced under subsequent negative R cycling.

4 Conclusion

- Lap joint of 6061 aluminum alloy (2 mm) to a zinc coated steel sheet (1 mm) could be successfully made by the FSW process and failure load as high as 71.4 % of steel base metal could be achieved.
- 1000 rpm 50 mm min^{-1} has higher fatigue strength than 500 rpm 100 mm min^{-1} combination of parameter.
- Fatigue fracture occurred at the aluminium steel interface irrespective of load applied in case of 500 rpm 100 mm min^{-1} combination of parameter.
- While fracture location changed with load applied in case of 1000 rpm 50 mm min^{-1}. At 80 and 60 % load amplitude, fatigue fracture occurred at the aluminium-steel interface. Whereas, at 40 and 30 % of load amplitude crack at first propagates through the partially bonded joint line and ultimately shifts towards the aluminium side without entering at the stir zone.

- For both the parameters i.e. 1000 rpm 50 mm min^{-1} and 500 rpm 100 mm min^{-1} with negative R ratio i.e. −0.3 and −0.5 have decreased the fatigue life at 20 % of load amplitude, whereas fatigue life remains unaltered at 10^6 with R ratio of 0.3 and 0.5 at 20 % of load amplitude for both the joints.

References

1. DebRoy T, and Bhadeshia H K D H, *Sci Technol Weld Join* **15** (2010) 266.
2. Barnes T A, and Pashby I R, *J Mater Process Technol* **99** (2000) 62.
3. Park S H C, Sato Y S, and Kokawa H, in *Proc 7th Int Symp*, Kobe, Japan, JWS (2001), p 639.
4. Ryabov V R, *Foreign Technology Division*, Wright Patterson airforce base, Ohio (1973).
5. Elrefaey A, Gouda M, Takahashi M, and Ikeuchi K, *J Mater Eng Perform* **14** (2005) 10.
6. Maruzen (ed), *Welding Handbook*, Japan Welding Society, Tokyo (1990), p 496.
7. Aritoshi M, and Okita K, *Q J Jpn Weld Soc* **71** (2002) 432.
8. Lee W, Schmuecker M, Mercardo U A, Biallas G, and Jung S, *Scr Mater* **55** (2006) 355.
9. Tanaka K, Kumagai M, and Yoshida H J, *Jpn Inst Light Met* **56** (2006) 317.
10. Kimapong K, and Watanabe T, *Mater Trans JIM* **46** (2005) 835.
11. Watanabe T, Takayama H, and Yanagisawa A, *J Mater Process Technol* **178** (2006) 342.
12. Chen Y C, and Nakata K, *Met Mater Trans A* **39A** (2008) 1985.
13. Uzun H, Donne C D, Argagnotto A, Ghidini T, and Gambaro C, *Mater Design* **26** (2005) 41.
14. Bozzi S, Etter A L H, Baudin T, Criqui B, and Kerbiguet J G, *Mater Sci Eng A* **527** (2010) 4504.
15. Das H, Basak S, Das G, and Pal T K, *Int J Adv Manuf Technol* **64** (2013) 1653.
16. Das H, Jana S S, Pal T K and De A, *Sci Technol Weld Join* **19** (2014) 69.
17. Biallas G, Dalle Donne C, and Juricic C, in *Advances in Mechanical Behaviour Plasticity and Damage. Proceedings of EUROMAT 2000*, vol. 1, (eds) Miannay D, Costa P, Francois D, Elsevier, Amsterdam (2000), p 115.
18. Braun R, Biallas G, Dalle Donne C, and Staniek G, in *Materials for Transportation Industry EUROMAT'99*, vol. 1, (ed) Winkler P-J, Wiley, Weinheim (2000), p 150.
19. Dalle Donne C, and Biallas G, *Fatigue and Fracture Performance of Friction Stir Welded 2024-T3 Joints*. European conference on spacecraft structures materials and mechanical testing, Braunschweig, Germany (1998).
20. Dawes C, and Thomas W, *Friction Stir Welding of Aluminium Alloy*. TWI reprint 493/6/95, Bulletin 6 (1995).
21. Ericsson M, Sandsttöm R, and Hagström J, *Fatigue of Friction Stir Welded AlMgSi-Alloy 6082. Second international symposium on FSW*, Gothenburg, Sweden (2000).
22. Hagström J, and Sandström R, *Fatigue Properties of Welded Joints in Extruded AlMgSi-Alloys*. Internal report. Department of Materials Science and Engineering, Royal Institute of Technology, S-100 44 Stockholm, Sweden, KTH/AMT-168, ISSN 0282-9770 (1997).
23. Kawasaki T, Makino T, Todori S, Takai H, Ezumi M, and Ina Y, *Application of Friction Stir Welding to the Manufacturing of Next*

Generation 'A-train' Type Rolling stock, Second international symposium on FSW, Gothenburg, Sweden (2000).

24. Magnusson L, and Kallman L, *Mechanical Properties of Friction Stir Welds in Thin Sheet of Aluminium 2024, 6013 and 7475.* Second international symposium on FSW, Gothenburg, Sweden (2000).

25. Okura I, Naruo M, Vigh L G, Hagisawa N, and Toda H, *Fatigue of Aluminium Deck Fabricated by Friction Stir Welding.* Eighth international conference INALCO (2001).

26. Lomolino S, *Fatigue strength and mechanical properties of butt joints FS welded on 6056-T4 Al-alloy.* GKSS internal report. GKSS Forschungszentrum Geesthacht, Germany (2001).

27. Tovo R, De Sisciolo R, and Volpone M, *Proprieta' Meccaniche e Microstrutturali di Giunti 'Fiction Stir Welded' in Lega d'Alluminio.* XXIX Convegno Nazionale AIAS, Lucca, Italia (2000).

28. Dalle Donne C, Raimbeaux G, Biallas G, Allehaux D, Palm F, and Ghidini T, *Fatigue Properties of Friction Stir Welded Aluminium Butt Joints*, ICAF 2003—fatigue of aeronautical structures as an engineering challenge (2003).

29. Dickerson T L, *Int J Fatigue* **25** (2003) 1399.

30. Ericsson M, and Sandström R, *Int J Fatigue* **25** (2003) 1379.

31. James M N, and Bradley G R, *Int J Fatigue* **25** (2003) 1389.

32. Zhou C, Yang X, and Luan G, *Scr Mater* **53** (2005) 1187.

33. Lomolino S, Tovo R, and Dos Santos J, *Int J Fatigue* **27** (2005) 305.

34. Cavaliere P, Campanile G, Panella F, and Squillace A, *J Mat Process Technol* **180** (2006) 263.

35. Scialpi A, De Giorgi M, De Filippis L A C, Nobile R, and Panella F W, *Mater Design* **29** (2008) 928.

36. Das H, Chakraborty D, and Pal T K, *Trans Nonferrous Met Soc China* **24** (2014) 648.

37. Moreira P M G P, Figuiredo M A V de, and Castro P M S T de, *Theor Appl Fract Mech*, **48** (2007) 169.

38. Niendorf T, Canadinc D, Maier H J, and Karaman I. *Int J Fatigue* **30** (2008) 426.

39. Fredriksson K, Melander A, and Hedman M, *Int J Fatigue* **10** (1988) 139.

40. Biswas K, Elsing L, Gorl E, and Schulte M, *Steel Res Int* **64** (1993) 407.

41. Biswas K, Hauman W, and Schulte M, *Technische Mitteilungen Krupp (English Edition)* **1** (1994) 33.

42. Zimmer S, Langlois L, Laye J, and Bigot R, *Int J Adv Manuf Technol* **47** (2010) 201.

43. Das H, Ghosh R N, and Pal T K, *Met Mater Trans A* **45A** (2014) 5098.

44. Stephens R I, Chen D K, and Hom B W, *ASTM STP 595*, American Society for Testing and Materials, Philadelphia (1976), p 27.